plausible scheme to produce the observed momentum correlation of the electrons.

Our measured momentum correlation shows that it is not the electron correlation in the initial ground state of the atom that leads to the enhanced double ionization in strong fields, but rather a re-scattering which is a result of the driving field. The magnitude of the momenta of the electrons in the direction of the laser field provides information on the phase of the field at the instant of recollision. The width of the distribution in the k^- direction is sensitive to the details of the re-scattering. Thus we expect that the momentum in the k^- direction and the momentum correlation in the directions perpendicular to the polarization will give further insight into the details of the correlation mechanism in future studies.

Finally, we note that the observed emission of the electrons to the same side confirms a prediction of Taylor *et al.*[28]. They have solved the time-dependent Schrödinger equation for two electrons in an optical field in three dimensions and found that most of the double ionization probability flux emerges to the same side. Similar conclusions have been drawn from one-dimensional model calculations[29,30].

The findings of this work provide a benchmark for theoretical efforts to calculate one of the most simple correlated two-electron processes in nature. Our method, using many-particle momentum space imaging for strong field physics, opens up the road for a variety of applications. The study of electron correlation in strong fields is now possible in molecules, clusters and solids (such as superconductors). □

Received 13 January; accepted 17 March 2000.

1. Briggs, J. S. & Schmidt, V. Differential cross sections for photo-double-ionization of the helium atom. *J. Phys. B* **33,** R1–R48 (2000).
2. Moshammer, R. *et al.* Double ionization of helium and neon for fast heavy-ion impact: Correlated motion of electrons from bound to continuum states. *Phys. Rev. Lett.* **77,** 1242–1245 (1996).
3. Lambropoulos, P., Maragakis, P. & Zhang, J. Two-electron atoms in strong fields. *Phys. Rep.* **305,** 203–293 (1998).
4. Fittinghoff, D. N., Bolton, P. R., Chang, B. & Kulander, K. C. Observation of nonsequential double ionization of helium with optical tunneling. *Phys. Rev. Lett.* **69,** 2642–2645 (1992).
5. Walker, B. *et al.* Precision measurement of strong field double ionization of helium. *Phys. Rev. Lett.* **73,** 1227–1231 (1994).
6. Corkum, P. B. Plasma perspective on strong field multiphoton ionization. *Phys. Rev. Lett.* **71,** 1994–1997 (1993).
7. Kulander, K. C., Cooper, J. & Schafer, K. J. Laser-assisted inelastic rescattering during above threshold ionization. *Phys. Rev. A* **51,** 561–568 (1995).
8. Liu, W. C., Eberly, J. H., Haan, S. L. & Grobe, R. Correlation effects in two-electron model atoms in intense laser fields. *Phys. Rev. Lett.* **85,** 520–523 (1999).
9. Watson, J. B., Sanpera, A., Lappas, D. G., Knight, P. L. & Burnett, K. Nonsequential double ionization of helium. *Phys. Rev. Lett.* **78,** 1884–1887 (1997).
10. Lappas, D. G. & van Leeuwen, R. Electron correlation effects in the double ionization of He. *J. Phys. B* **31,** L249–256 (1998).
11. LaGattuta, K. J. & Cohen, J. S. Quasiclassical modelling of helium double photoionisation. *J. Phys. B* **31,** 5281–5291 (1998).
12. Becker, A. & Faisal, F. H. M. Mechanism of laser-induced double ionization of helium. *J. Phys. B* **29,** L197–202 (1996).
13. Becker, A. & Faisal, F. H. M. S-matrix analysis of ionization yields of noble gas atoms at the focus of Ti:sapphire laser pulses. *J. Phys. B* **32,** L335–L343 (1999).
14. Schafer, K. J., Yang, B., DiMauro, L. F. & Kulander, K. C. Above threshold ionization beyond the high harmonic cutoff. *Phys. Rev. Lett.* **70,** 1599–1602 (1993).
15. Fittinghoff, D. N., Bolton, P. R., Chang, B. & Kulander, K. C. Polarization dependence of tunneling ionization of helium and neon by 120-fs pulses at 614 nm. *Phys. Rev. A* **49,** 2174–2177 (1994).
16. Sheehy, B., Lafon, R., Widmer, M., Walker, B. & DiMauro, L. F. Single- and multiple-electron dynamics in the strong-field tunneling limit. *Phys. Rev. A* **58,** 3942–3952 (1998).
17. Becker, A. & Faisal, F. H. M. Interplay of electron correlation and intense field dynamics in the double ionization of helium. *Phys. Rev. A* **59,** R1742–R1745 (1999).
18. Weber, T. *et al.* Recoil-ion momentum distributions for single and double ionization of helium in strong laser fields. *Phys. Rev. Lett.* **84,** 443–446 (2000).
19. Weber, T. *et al.* Sequential and nonsequential contributions to double ionization in strong laser fields. *J. Phys. B* **33,** L128–L133 (2000).
20. Moshammer, R. *et al.* Momentum distributions of Ne ions created by an intense ultrashort laser pulse. *Phys. Rev. Lett.* **84,** 447–450 (2000).
21. Dörner, R. *et al.* Cold target recoil ion momentum spectroscopy. *Phys. Rep.* **330,** 95–192 (2000).
22. Ullrich, J. *et al.* Cold target recoil ion momentum spectroscopy. *J. Phys. B* **30**, 2917–2974 (1997).
23. Dörner, R. *et al.* Photo double ionization of He: Fully differential and absolute electronic and ionic momentum distributions. *Phys. Rev. A* **57,** 1074–1090 (1998).
24. DiMauro, L. F. & Agostini, P. in *Advances in Atomic and Molecular Physics* 79–120 (Academic, New York, 1995).
25. Larochelle, S., Talebpour, A. & Chin, S. L. Non-sequential multiple ionization of rare gas atoms in a Ti:Sapphire laser field. *J. Phys. B* **31,** 1201–1214 (1998).
26. Becker, A. & Faisal, F. H. M. Interpretation of momentum distribution of recoil ions from laser induced non-sequential double ionization. *Phys. Rev. Lett.* **84,** 3546–3549 (2000).
27. Dörner, R. *et al.* Fully differential cross sections for double photoionization of He near threshold measured by recoil ion momentum spectroscopy. *Phys. Rev. Lett.* **77,** 1024–1027 (1996).
28. Taylor, K. T., Parker, J. S., Dundas, D., Smyth, E. & Vitirito, S. Laser driven helium in full-dimensionality. *Laser Phys.* **9,** 98–116 (1999).
29. Lein, M., Gross, E. K. U. & Engel, V. On the mechanism of strong-field double photoionisation in the helium atom. *J. Phys. B* **33,** 433–442 (2000).
30. Dörr, M. Double ionization in a one-cycle laser pulse. *Optics Express* **6,** 111–116 (2000).

Acknowledgements

We thank H. Schmidt-Böcking for enthusiastic support, and R. Moshammer and J. Ullrich for helpful discussons. Our analysis of the influence of the laser field on the final state momenta emerged after fruitful discussion with A. Becker and F. H. M. Faisal. We are grateful to W. W. Rühle for continuous support and thank Roentdek GmbH for providing the position sensitive detectors. This work is supported by DFG, BMBF, GSI and DAAD. R.D. is supported by the Heisenberg Programme of the DFG. The Marburg group thanks the Land Hessen and the DFG for support through the SFB383 and their Graduierten-kolleg 'Optoelektronik mesoskopischer Halbleiter'.

Correspondence and requests for materials should be addressed to R.D. (e-mail: doerner@hsb.uni-frankfurt.de).

Improving the performance of doped π-conjugated polymers for use in organic light-emitting diodes

Markus Gross*, David C. Müller*, Heinz-Georg Nothofer†, Ulrich Scherf†, Dieter Neher‡, Christoph Bräuchle* & Klaus Meerholz*

** Institut für Physikalische Chemie, Ludwig-Maximilian-Universität München, Butenandtstrasse 11, 81377 München, Germany*
† Max-Planck Institute für Polymerforschung, Institut Ackermannweg 10, 55037 Mainz, Germany
‡ Institut für Experimentalphysik, Universität Potsdam, Am Neuen Palais 10, 14469 Potsdam, Germany

Organic light-emitting diodes (OLEDs) represent a promising technology for large, flexible, lightweight, flat-panel displays[1–3]. Such devices consist of one or several semiconducting organic layer(s) sandwiched between two electrodes. When an electric field is applied, electrons are injected by the cathode into the lowest unoccupied molecular orbital of the adjacent molecules (simultaneously, holes are injected by the anode into the highest occupied molecular orbital). The two types of carriers migrate towards each other and a fraction of them recombine to form excitons, some of which decay radiatively to the ground state by spontaneous emission. Doped π-conjugated polymer layers improve the injection of holes in OLED devices[4–9]; this is thought to result from the more favourable work function of these injection layers compared with the more commonly used layer material (indium tin oxide). Here we demonstrate that by increasing the doping level of such polymers, the barrier to hole injection can be continuously reduced. The use of combinatorial devices allows us to quickly screen for the optimum doping level. We apply this concept in OLED devices with hole-limited electroluminescence (such as polyfluorene-based systems[10–12]), finding that it is possible to significantly reduce the operating voltage while improving the light output and efficiency.

OLED devices are typically fabricated using one transparent electrode. The material most commonly employed for this purpose is indium tin oxide (ITO), which serves as the anode. The electronic work function ϕ_w of ITO is generally smaller than the highest

occupied molecular orbital (HOMO) level of most organic semiconductors, resulting in a barrier φ_h for hole injection. The work function of ITO has been shown to depend strongly on the manufacturing process and any pretreatment[13,14], which makes the reproducibility of device fabrication rather difficult. Heeger *et al.*[5] have shown that coating the ITO with "doped" (that is, oxidized) polyaniline reduced φ_h and, consequently, lowered the onset voltage and operating voltage of the devices. More recently, polypyrrole (ref. 6) and most importantly poly(3,4-ethylenedioxythiophene) (PEDOT) have been used as the injection layer for holes[7–9]. We note that counter ions are needed for compensation of the charges of the oxidized π-conjugated polymer; such counter ions might also have a considerable influence. In the case of commercially available PEDOT, the polyanion poly(styrene sulphonate) (PSS) is commonly used.

All studies using π-conjugated polymeric anodes for OLED applications have so far neither reported nor taken into account the exact doping level of the polymer, though it has long been known that the latter is correlated with the electrochemical equilibrium potential of the polymer, E_{eq} (ref. 15). Generally, a simple offset of 4.45 eV is assumed to exist between electrochemical potentials and distinct energy levels such as the work function (ϕ_w) (refs 10, 16). Ultraviolet Photon Spectroscopy (UPS) measurements performed on two differently synthesized PEDOT samples yielded ϕ_w values of ~4.0 eV for 'neutral' and 4.4 eV for 'doped' material, respectively[17]. More recently, $\phi_w = 5.2$–5.3 eV was determined by electroabsorption and the Kelvin-probe method[18]. These large variations may not only be caused by the different methods, but probably also stem from differences in the film preparation leading to different degrees of oxidation (work function) of the PEDOT. Because ϕ_w directly influences the barrier φ_h, strong variations in the OLED performance are expected.

These considerations clearly indicate that variations in the degree of oxidation might be one of the possible sources for the irreproducible performance of OLED devices using polymeric hole-injection contacts. On the other hand, they also suggest that it should be possible to actively influence ϕ_w of such anodes by adjusting the doping level of the polymer. The particular advantage of π-conjugated polymers for this purpose is that they are generally redox-active over a broad potential range[15]. Within this range, a continuous distribution of redox states is observed as is clearly evident from the cyclic voltammogram in Fig. 1a. Thus, the work function ϕ_w should be adjustable in infinitesimally small steps within the redox-active range by either electrochemical or chemical means.

Here we introduce poly(4,4′-dimethoxy-bithiophene) (PDBT, inset Fig 1a) as a 'new' hole-injection contact material for OLEDs, because it offers several advantages over other π-conjugated polymers: (1) it is the most stable conjugated polymer known to date,

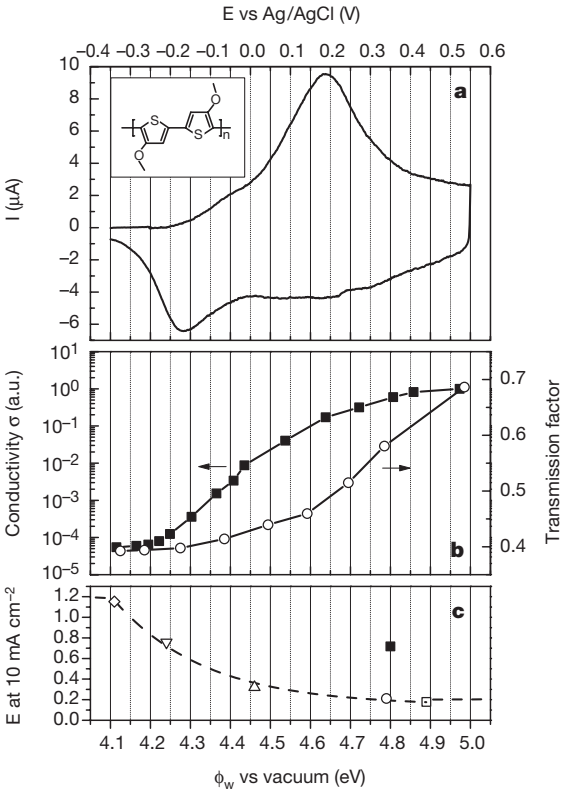

Figure 1 Electrochemical and electro-optical properties of PDBT and its performance as the hole injection contact of hole-only OLED devices. **a**, Cyclic voltammogram of a PDBT film deposited on ITO, which served as the working electrode, in the section of interest for this study. The measurement was performed in a 0.1 M tetrabutylammonium hexafluorophosphate/acetonitrile solution. The upper *x* axis shows the work function ϕ_w versus the vacuum level. The offset between the two axes is 4.45 eV (ref. 16). Note that variations of ϕ_w cannot be achieved with PDBT below 4.1 eV due to the absence of redox couples (no current in the cyclic voltammogram). Inset, chemical structure of PDBT. **b**, Conductivity σ (filled squares, left axis) and transmission factor for PFO emission (open circles, right axis) of 150-nm PDBT films as a function of the adjusted potential E_{eq}/work function ϕ_w. The relative conductivity σ was obtained by investigation of a PDBT film deposited on a pair of interdigitated electrodes. For each particular data point, the film was adjusted to a certain redox potential in an acetonitrile/NaPSS solution, dried, and then the impedance (equivalent to resistance for low frequency) was determined by measuring the voltage drop on a calibrated resistor in series with the film by use of a lock-in amplifier. The total applied a.c. voltage was 10 mV and the frequency was 4 Hz. The data were normalized to the value obtained for $E_{eq} = +0.53$ V. The transmission factor was obtained by convolution of each individual absorption spectrum for a given E_{eq} with the EL spectrum of PFO (inset Fig. 3b), integration, and finally normalization with the integrated EL spectrum through ITO. The absorption spectra of PDBT were measured *in situ* in a transmission electrochemical cell as a function of E_{eq}. **c**, Electric field necessary to pass a current of 10 mA cm^{-2} through the 'hole-only' devices with the general structure anode/hole-transport layer/Al determined from the data in Fig. 2. This field is plotted against the adjusted potential E_{eq}/work function ϕ_w for the devices with different PDBT injection layers (open symbols) and the device using a PEDOT anode (filled square). E_{eq} was determined before spin-casting the hole-transport layer. The dashed line is a guide to the eye.

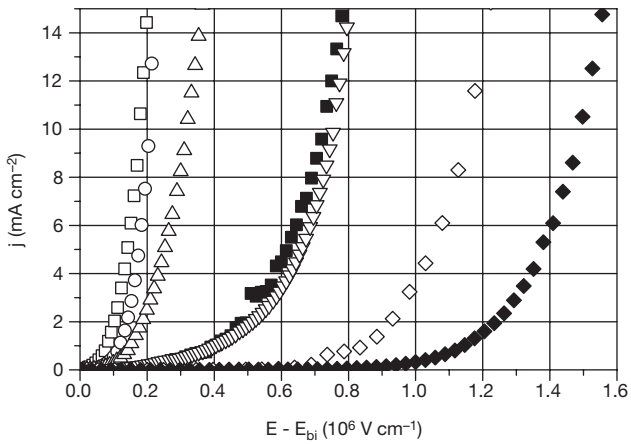

Figure 2 I–V characteristics of hole-only devices with differently doped PDBT injection–contacts. The figure shows the field dependence of the electric current density *j* for various devices with the general structure anode/hole-transport layer/Al. PDBT devices adjusted to different electrochemical potentials E_{eq}/work functions ϕ_w (open symbols): $E_{eq} = +0.44$ V (squares), +0.34 V (circles), +0.01 V (up triangles), –0.21 V (down triangles), and –0.34 V (diamonds). PEDOT device with $E_{eq} = 0.36$ V (filled squares) and plain ITO device (filled diamonds). All E_{eq} values are given versus the reference electrode Ag/AgCl. The polymeric anodes were 40–50 nm thick, the hole-transport layer 200-nm thick. In all cases, the voltage actually applied (or electric field) was corrected for the built-in potential V_{bi} resulting from the different work functions of the two contact electrodes[18,21].

that is, it is in principle fully oxidizable (one charge per thiophene unit) without chemical degradation[19]; (2) it offers an extremely wide range of tunability for the electrochemical equilibrium potential E_{eq} of between −0.4 V and +2.5 V versus Ag/AgCl (ref. 19) ($4.05\,eV < \phi_w < 6.95\,eV$; note that Fig. 1a only shows the section of interest for this study). Additionally, PDBT is almost transparent to visible light in the doped state, and exhibits electrical conductivity $\sigma > 100\,S\,cm^{-1}$.

We employed three kinds of hole-injecting anodes in our devices: (1) ITO (20 Ω per square), (2) PEDOT films on ITO-coated substrates spin-coated from an aqueous suspension ("Baytron P", Bayer Corporation), and (3) PDBT films oxidized at different redox potentials. The latter were deposited onto ITO-coated substrates by electropolymerization of the 'monomer', 4,4′-dimethoxybithiophene, at 1.2 V in a saturated water/acetonitrile 1:1 solution containing sodium poly(styrene sulphonate) (NaPSS, Aldrich; molecular mass, 70,000 g mol^{-1}) as the supporting electrolyte. After preparation, the degree of oxidation of the PDBT films was adjusted electrochemically to different values in a monomer-free acetonitrile/NaPSS solution. Thereafter, the films were carefully rinsed with acetonitrile and water. Finally, all substrates were dried at 80 °C in vacuum. The equilibrium potential E_{eq} was determined after this entire procedure (accuracy ±0.05 V). For device fabrication, the organic layers were deposited by spin-casting the appropriate solutions onto the as-prepared substrates and then dried in vacuum. We note that PEDOT and PDBT are both insoluble after film formation. Finally, a top electrode was evaporated, yielding diodes with an active area of 9.1 mm^2. All devices were characterized in nitrogen atmosphere.

Previous studies using π-conjugated polymers as the hole-injecting anode were restricted to the doped (that is, conductive) state of those polymers, and it was demonstrated that the OLED performance is independent of the thickness of the conjugated polymer[4–9]. Therefore, it was considered as part of the injection contact. However, it is well-known that the conductivity σ of conjugated polymers generally varies for different doping levels[15], which has to be taken into account, in particular for the state of low conductivity. For PDBT, σ decreases over four orders of magnitude upon discharging (Fig. 1b), but despite this we did not observe a strong influence of the uncharged PDBT layer thickness on the I–V curves. Nevertheless, to keep this ambiguity as small as possible, the PDBT layer was generally less than one-third the thickness of the following semiconducting layer(s).

First, we studied the influence of the anode material on the I–V characteristics in single-layer 'hole only' devices. They consisted of a hole-transport layer containing 50 wt% of *N*,*N*′-diphenyl-*N*,*N*′-(3-methylphenyl)-1,1′-biphenyl-4,4′-diamine (TPD; Syntec GmbH) dispersed in polycarbonate (Aldrich; molecular mass, 64,000 g mol^{-1}). Aluminum served as the cathode. None of the devices showed electroluminescence (EL) due to the negligibly small number of electrons. As expected the ITO device showed a higher current onset field than all devices using polymeric anodes (Fig. 2), a fact which is typically attributed to the more favourable work function[4–9]. Within the series of devices using a PDBT anode, the onset field for hole injection decreases systematically with increasing oxidation potential E_{eq}. Any intermediate performance level not specifically shown can be obtained by properly adjusting E_{eq}. As the hole-transport layer is identical in all cases, these observations must be correlated with a decreased barrier φ_h as a result of increased work function ϕ_w of the PDBT. They constitute an indirect, but unambiguous, proof for the feasibility of our concept of influencing the work function by adjusting the redox state of a conjugated polymer.

Due to the lack of suitable analytical models describing charge-injection into amorphous organic semiconductors, an exact and quantitative evaluation of the data is at present not possible. Instead, we plotted the field necessary to pass a certain current density through the devices (for example, 10 mA cm^{-2}) as a function

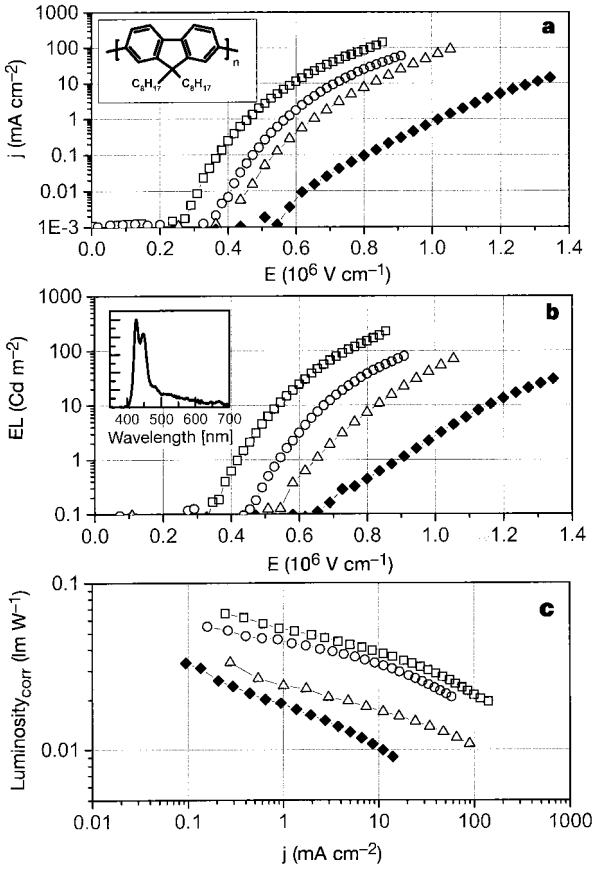

Figure 3 Performance of various OLED devices with the general structure anode/PFO/Ca. Results are shown for PDBT devices adjusted to different electrochemical potentials E_{eq}/work functions ϕ_w (open symbols): $E_{eq} = +0.30$ V (squares), −0.05 V (circles) and −0.25 V (up triangles); ITO reference device (filled diamonds). All E_{eq} values are given versus the reference electrode Ag/AgCl. The polymeric anodes were 150-nm thick, and the hole-transport layer was 550-nm thick. **a**, Field dependence of the electric current density *j*. Inset, chemical structure of PFO. **b**, Field dependence of the light output (EL). Inset, emission spectrum of PFO. **c**, Current dependence of the luminosity.

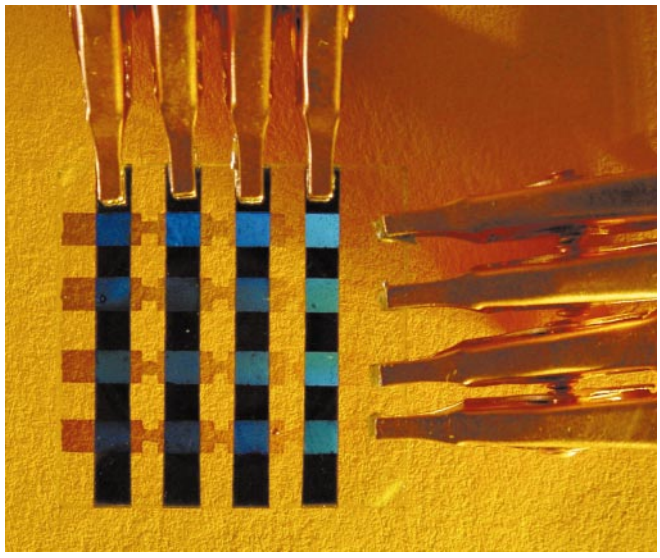

Figure 4 Two-dimensional combinatorial OLED array. The PDBT thickness increases top to bottom; the electrochemical equilibrium potential increases left to right. See text for details.

of E_{eq} (ϕ_w; see Fig. 1c). It can be seen that this field (E at 10 mA cm^{-2}) decreases dramatically with increasing E_{eq}, and levels off before reaching the HOMO level of TPD (5.07 eV, determined electrochemically in solution). This indicates that even though there should still be a considerable energy barrier between the HOMO of TPD and the work function of the highly-doped PDBT, an ohmic contact has almost been achieved. This is in agreement with a recent theoretical study[20] predicting ohmic contacts for energy barriers smaller than 0.3 eV. Charge injection in the PEDOT reference device (E_{eq}(PEDOT) = +0.36 V) was consistently more difficult than in the PDBT device displaying a similar E_{eq} of the anode layer. These results indicate that the work function is not the only factor influencing carrier injection and performance of OLED devices. The discrepancy might result from the different preparation methods of the PEDOT and PDBT films (spin-coating of the suspension versus electrochemical deposition), or might be due to the different substituents at the thiophene ring (ethylenedioxy ring versus methoxy group). Note that the dopant counter ions were identical in both cases (PSS).

Because the onset field decreases, and density of holes at a given field increases, with increasing doping level (E_{eq}, ϕ_w) of the PDBT, this should have a very marked effect on the performance of OLED devices. We distinguish two cases; (1) devices with an excess number of holes in the emission layer and (2) hole-deficient devices. A typical example of the more-common first case are single-layer poly(2-methoxy, 5-(2′-ethyl-hexyloxy)-1,4-phenylenevinylene) (MEH-PPV) devices. Here, the increase of the doping level of the PDBT anode led to an even further increased hole current at a given field, while the brightness remained basically unchanged. Overall, this yielded a reduction of the efficiency (M.G., D.C.M. and K.M., unpublished results). To study the opposite case (2), we selected 9,9-bis(n-octyl)fluorene (PFO) as the emitting layer, and again simple one-layer devices were fabricated. PFO has the HOMO at 5.8 eV, giving rise to a large barrier for hole injection from ITO[10,11]. Calcium was evaporated as the electron-injecting cathode.

All devices showed blue electroluminescence with a maximum wavelength of 436 nm, similar to results reported in ref. 10 (inset Fig. 3). As expected, the onsets of the current and the light output both decrease monotonously with increasing E_{eq} (ϕ_w) of the PDBT anode (Fig. 3). For a given electric field, the EL increases by more than one order of magnitude in the devices using charged PDBT compared with those using non-charged PDBT and even more than two orders of magnitude compared with the ITO reference device despite absorption losses in the PDBT layer (Fig. 1b). Within the series of PDBT devices, the best external light output of 250 Cd m^{-2} was achieved with the highly-doped PDBT device with an external efficiency of $\eta_{ext} = 0.18$ Cd A^{-1}. Taking into account the absorption of the PDBT (Fig. 1b), this corresponds internally to $\eta_{corr} \approx 0.33$ Cd A^{-1}, which is comparable to the values for a bilayer device using a "TPD-polymer" as hole-transporting layer[10].

In Fig. 3c, the luminosity (as a measure for the energy conversion efficiency of the OLED) is plotted as a function of current. For better comparison, the EL data have been corrected for variations of the PDBT transmission (see Fig. 1b), which generally accompany the change of the redox state in π-conjugated polymers[15]. The luminosity of the PDBT devices is dependent on E_{eq}, and is a factor ~2.5 times higher in the highly-doped PDBT device than in the slightly-doped case and ~4 times higher than for the ITO reference for the same current density (for example, 10 mA cm^{-2}). This shows that the enhanced hole injection not only reduces the onset voltage, but also influences the recombination efficiency positively due to the more balanced number density of the two carrier types inside the luminescent layer. On the other hand, for a given electric field (such as $E = 0.8$ MV cm^{-1}) the luminosity exhibits an intermediate optimum value. We attribute the decreased luminosity for higher ϕ_w to enhanced heating phenomena.

We have shown that 'hole-only' and OLED devices using highly-doped PDBT anodes showed strongly reduced onset fields compared to those using non-doped PDBT, ITO or commercially available PEDOT as the anode. Furthermore, the luminosity in OLEDs based on a polyfluorene derivative, that is, with hole-limited EL, was increased. Similar observations have been obtained with a number of materials with very different HOMO levels, including various composites and emissive conjugated polymers. Our concept thus opens up the possibility of optimizing devices by properly adjusting the work function of the polymeric anode. We point out that this is not restricted to PDBT, but may be used with π-conjugated polymers in general. The alternative way to influence charge injection into a certain organic semiconductor is the introduction of additional transport layer(s). Normally, several layers are necessary to cause the barrier to vanish, and ultimately higher voltages are required, reducing the power efficiency.

We have used electrochemistry for screening purposes, even though it is possible to achieve similar results by chemical oxidation/reduction processes. But electrochemistry is more convenient, as it simultaneously offers the possibility of (1) depositing the polymer onto the ITO, (2) adjusting the degree of oxidation in infinitesimally small steps by simply changing the 'oxidation power' of the working electrode, and (3) determination of E_{eq} before deposition of the other organic layers. Furthermore, combinatorial devices can easily be fabricated, greatly reducing the time necessary for device optimization. Each device on one substrate can be adjusted independently to a different E_{eq} by means of electrochemistry. An example of a two-dimensional combinatorial array is shown in Fig. 4. In the first dimension, the redox state is varied, and in the second dimension, the thickness of the polymeric anode material is changed. Alternatively, various injection polymers with identical E_{eq} could be tested, and so on. Once the optimum doping level is known, the conditions for achieving this specific doping level by chemical methods have to be explored to make our approach applicable for preparation of these films on a large scale in an industrial environment.

It should be possible to extend this principle, which is presented here for hole injection only, to electron injection. Our concept also opens the way to various new possibilities for tuning and structuring displays. For example, it could perhaps be used to fabricate monochrome 'grey-level' displays by adjusting to different redox states the specific areas of a substrate covered uniformly with PDBT. Due to the locally varying hole currents, the luminescent layer would then emit light with different brightnesses. □

Received 3 February; accepted 20 April 2000.

1. Friend, R. H. *et al.* Electroluminescence in conjugated polymers. *Nature* **397,** 121–128 (1999).
2. Heeger, A. J. Light emission from semiconducting polymers: light-emitting diodes, light-emitting electrochemical cells, lasers and white light for the future. *Solid State Commun.* **107,** 673–679 (1998).
3. Salbeck, J. Electroluminescence with organic compounds. *Ber. Bunsenges. Phys. Chem.* **100,** 1667–1677 (1996).
4. Gustafsson, G. *et al.* Flexible light-emitting diodes made from soluble conducting polymers. *Nature* **357,** 477–479 (1992).
5. Yang, Y. & Heeger, A. J. Polyaniline as a transparent electrode for light-emitting diodes: Lower operating voltage and higher efficiency. *Appl. Phys. Lett.* **64,** 1245–1247 (1994).
6. Gao, J., Heeger, A. J., Lee, Y. J. & Kim, C. Y. Soluble polypyrrole as the transparent anode in polymer light-emitting diodes. *Synth. Met.* **82,** 211–223 (1996).
7. Carter, S. A., Angelopoulos, M., Karg, S., Brock, P. J. & Scott, J. C. Polymeric anodes for improved polymer light-emitting diode performance. *Appl. Phys. Lett.* **70,** 2067–2069 (1997).
8. Scott, J. C., Carter, S. A., Karg, S. *et al.* Angelopoulos, M. Polymeric anodes for light-emitting diodes. *Synth. Met.* **85,** 1197–1200 (1997).
9. Cao, Y., Yu, G., Zhang, C., Menon, R. & Heeger, A. J. Polymer light-emitting diodes with polyethylene dioxythiophene-polystyrene sulfonate as the transparent anode. *Synth. Met.* **87,** 171–174 (1997).
10. Grice, A. W. *et al.* High brightness and efficient blue light-emitting polymer diodes. *Appl. Phys. Lett.* **73,** 629–631 (1998).
11. Janiez, S. *et al.* Electrochemical determination of the ionization potential of poly(9,9-dioctylfluorene). *Appl. Phys. Lett.* **73,** 2453–2455 (1998).
12. Grell, M. *et al.* Polarized electroluminescence from a liquid crystalline polyfluorene. *Adv. Mater.* **11,** 671–674 (1999).
13. Nuesch, F., Rothberg, L. J., Forsythe, E. W., Quoc Toan, L. & Gao, Y. A. Photoelectron spectroscopy study on the indium tin oxide treatment by acids and bases. *Appl. Phys. Lett.* **74,** 880–882 (1999).
14. Kim, J. S. *et al.* Indium tin oxide treatments for single and double layer polymeric light emitting diodes. The relation between the anode physical, chemical, and morphological properties and the device performance. *J. Appl. Phys.* **84,** 6859–6870 (1998).

15. Skotheim, T. A. *Handbook of Conducting Polymers* (Dekker, New York, 1986).
16. Bard, A. J. & Faulkner, L. A. *Electrochemical Methods—Fundamentals and Applications* (Wiley, New York, 1984).
17. Xing, K. Z., Fahlman, M., Chen, X. W., Inganäs, O. & Salaneck, W. R. The electronic structure of poly(3,4-ethylene-dioxyghiophene): studied by XPS and UPS. *Synth. Met.* **89,** 161–165 (1997).
18. Brown, T. M. *et al.* Built-in field electroabsorption spectroscopy of polymer light-emitting diodes incorporating a doped poly(3,4-ethylene dioxythiophene) hole injection layer. *Appl. Phys. Lett.* **75,** 1679–1681 (1999).
19. Dietrich, M. & Heinze, J. Poly(4,4′-Dimethoxybithiophene)—A new conducting polymer with extraordinary redox and optical properties. *Synth. Met.* **41–43,** 503–506 (1991).
20. Malliaras, G. G. & Scott, J. C. Numerical simulations of the electrical characteristics and the efficiencies of single-layer organic light emitting diodes. *J. Appl. Phys.* **85,** 7426–7432 (1999).
21. Malliaras, G. G., Salem, J. R., Brock, P. J. & Scott, C. Electrical characteristics and efficiency of single-layer organic light-emitting diodes. *Phys. Rev. B* **58,** R13411–R13414 (1998).

Acknowledgements

We thank J. Heinze for making some bithiophene available, W. Brütting for discussions, and Bayer AG (Leverkusen, Germany) for the donation of Baytron P.

Correspondence and requests for materials should be addressed to K.M. (e-mail: klaus.meerholz@cup.uni-muenchen.de).

Selection of peptides with semiconductor binding specificity for directed nanocrystal assembly

Sandra R. Whaley*, D. S. English*, Evelyn L. Hu†, Paul F. Barbara*‡ & Angela M. Belcher*‡

** Department of Chemistry and Biochemistry, ‡ The Texas Materials Institute, The University of Texas at Austin, Austin, Texas 78712, USA*
†Center for Quantized Electronic Structures, University of California, Santa Barbara, California 93106, USA

In biological systems, organic molecules exert a remarkable level of control over the nucleation and mineral phase of inorganic materials such as calcium carbonate and silica, and over the assembly of crystallites and other nanoscale building blocks into complex structures required for biological function[1–4]. This ability to direct the assembly of nanoscale components into controlled and sophisticated structures has motivated intense efforts to develop assembly methods that mimic or exploit the recognition capabilities and interactions found in biological systems[5–10]. Of particular value would be methods that could be applied to materials with interesting electronic or optical properties, but natural evolution has not selected for interactions between biomolecules and such materials. However, peptides with limited selectivity for binding to metal surfaces and metal oxide surfaces have been successfully selected[10,11]. Here we extend this approach and show that combinatorial phage-display libraries can be used to evolve peptides that bind to a range of semiconductor surfaces with high specificity, depending on the crystallographic orientation and composition of the structurally similar materials we have used. As electronic devices contain structurally related materials in close proximity, such peptides may find use for the controlled placement and assembly of a variety of practically important materials, thus broadening the scope for 'bottom-up' fabrication approaches.

Phage-display libraries, based on a combinatorial library of random peptides—each containing 12 amino acids—fused to the pIII coat protein of M13 coliphage[12], provided us with $\sim 10^9$ different peptides that were reacted with crystalline semiconductor structures. Five copies of the pIII coat protein are located on one end of the phage particle, accounting for 10–16 nm of the particle. The phage-display approach provided a physical linkage between the peptide–substrate interaction and the DNA that encodes that interaction. The experiments described here utilized five different single-crystal semiconductors: GaAs(100), GaAs(111)A, GaAs(111)B, InP(100) and Si(100). These substrates allowed for systematic evaluation of the peptide–substrate interactions. Protein sequences that successfully bound to the specific crystal were eluted from the surface, amplified by 10^6, and re-reacted against the substrate under more stringent conditions. This procedure was repeated five times to select the phage with the most specific binding. After the third, fourth and fifth rounds of phage selection, crystal-specific phage were isolated and their DNA sequenced. We identified peptide binding that is selective for the crystal composition (for example, binding to GaAs but not to Si) and crystalline face (for example, binding to (100) GaAs, but not to (111)B GaAs).

Twenty clones selected from GaAs(100) were analysed to determine epitope binding domains to the GaAs surface. The partial peptide sequences of the modified pIII protein are shown in Fig. 1, revealing similar amino-acid sequences among peptides exposed to GaAs. With increasing number of exposures to a GaAs surface, the number of uncharged polar and Lewis-base functional groups increased. Phage clones from third, fourth and fifth round sequencing contained on average 30%, 40% and 44% polar functional groups, respectively, while the fraction of Lewis-base functional groups increased at the same time from 41% to 48% to 55%. The observed increase in Lewis bases, which should constitute only 34% of the functional groups in random 12-mer peptides from our library, suggests that interactions between Lewis bases on the peptides and Lewis-acid sites on the GaAs surface may mediate the selective binding exhibited by these clones.

The expected structure of the modified 12-mers selected from the library would be an extended conformation, which seems likely for

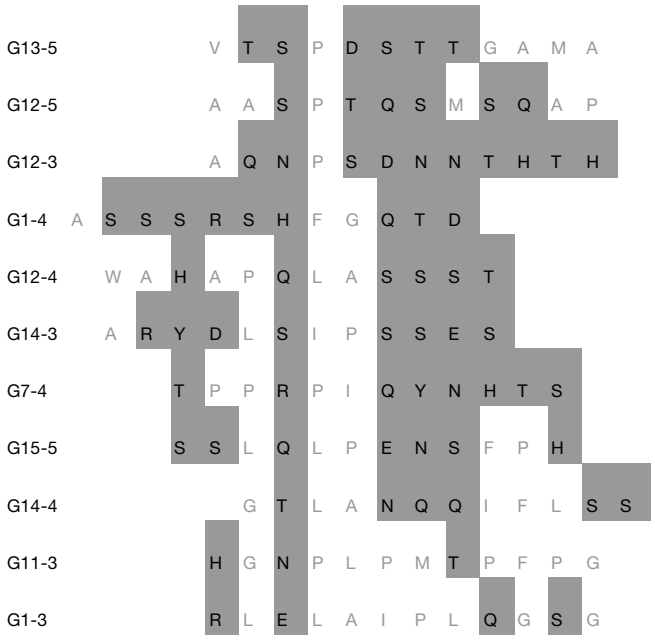

Figure 1 Selected amino-acid sequences of randomized peptide inserts. Here we show partial amino-acid sequences from clones that bound to GaAs(100). These sequences have amino acids with functional groups that can donate electrons to the GaAs surface (shaded areas). Serine (S) and threonine (T) both have hydroxyl side chains that differ by one carbon. Asparagine (N) and glutamine (Q) both have amine-bearing side chains that differ by one carbon. Non-polar amino acids are indicated by grey lettering. The clones were named as follows: G1-3 was the first clone selected from GaAs (100) during the third round of selection.